Computation and Spectroelectrochemistry as Complementary Tools for the Study of Electrochemically Induced Charged Defects in 4-[Bis(4-methylphenyl)amino]phenyl Oligothiophenes as Model Systems for Hole-Transporting Materials

J. Casado,[†] M. C. Ruiz Delgado,[†] Y. Shirota,[‡] V. Hernández,[†] and J. T. López Navarrete*,[†]

Departamento de Quimica Fisica, Facultad de Ciencias, Universidad de Malaga, Campus de Teatinos s/n, Malaga 29071, Spain, and Department of Applied Chemistry, Faculty of Engineering, Osaka University, Yamadaoka, Suita, Osaka 565-0871, Japan

Received: November 26, 2002

The in situ electronic absorption and Fourier transform Raman scattering spectra recorded during the electrochemical oxidation of two α,α′-end-capped 4-[bis(4-methylphenyl)amino]phenyl oligothiophenes with three and four thiophene rings are reported. We have characterized a radical cation and a dication species in the trimer and up to a radical trication in the tetramer. The electronic and the Raman spectra have been interpreted and assigned with the final goal of obtaining structural information about the contribution of the bis(4-methylphenyl)amino groups, the innermost phenyl rings, and the central thienyl chain length to the stabilization of the electrochemically induced charged defects. The experimental data have been supported by theoretical calculations in the framework of the density functional theory. The charged defects can be viewed as models of hole carriers or photoexcitons in real devices.

I. Introduction

The working state of a based-organic molecular device, such as light-emitting diodes (LEDs), memory devices, or field-effect transistors (FETs), involves several physicochemical processes in the material, namely, charge injection or photoexcitation, carrier transport (mobility) or charge recombination, and light emission in the case of the LED devices.[1−3] At a molecular level, charge injection, photoexcitation, and carrier recombination mainly depend on the ability of the molecules of stabilizing negative charges (electron injection) or positive charges (hole injection).

Oligothiophenes have attracted great attention because of their successful application as active materials in FETs and LEDs.[1−5] Although very recently oligothiophenes have been demonstrated to work as n-channel conductors in thin film transistors,[6] the majority of oligothiophenes can be viewed as rich electron systems and therefore addressed like p-channel conductor or hole-transporting materials.[1−5]

In this regard, one of us has reported the synthesis of new molecular materials consisting of a central oligothiophene moiety of variable length (up to a tetramer) α,α′-encapsulated with 4-[bis(4-methylphenyl)amino]phenyl groups (BMA-nT hereafter, see Figure 1 for chemical structures).[7−9] These oligothiophenes are thermally stable[10] hole-transporting materials with good film-forming properties and color tunability for LED applications. The capability of these materials for tunable emissions is directly related with the chain length and mainly with the π-electron delocalization over the thienyl backbone. At this point we refer to the reader for a more detailed vibrational spectroscopic study in ref 10 about the π-electron delocalization within the BMA-nT series.

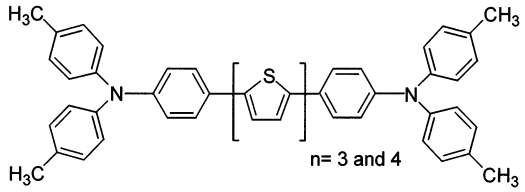

n=3, **BMA-3T**; n=4, **BMA-4T**.

Figure 1. Chemical structures of BMA-3T and BMA-4T.

In addition to molecular engineering aspects of active materials for molecular electronics or optoelectronics, the characterization at a molecular level of the charged defects as model of hole-active carriers or photoexcitons is needed to be considered in device design in order to improve their stability and their efficiency performance. Also these investigations are very useful for understanding the nature of the electron or photoelectron transfers in organic optoelectronic materials. In this work we will address a detailed spectroscopic study of all the stable charged defects created in BMA-3T and in BMA-4T which can be viewed as the hole carriers created in the real device. To this goal we will use in situ vis−NIR and in situ Raman spectroelectrochemical techniques: the absorption electronic bands will be related with the type of electronic defect, while from their Raman spectra meaningful information about the stabilizing interplay of the 4-[bis(4-methylphenyl)amino]-phenyl terminal (BMA) groups, the inner phenyl rings and the thiophene backbone will be extracted. This study will be supported and guided by theoretical calculations.

II. Experimental and Computational Details

Cell Description. Spectroelectrochemical in situ vis−NIR and Raman experiments were performed by using a locally prepared optically transparent thin layer electrode cell. The cell

* Corresponding author. E-mail: teodomiro@uma.es.
[†] Departamento de Quimica Fisica.
[‡] Department of Applied Chemistry.

10.1021/jp022484m CCC: $25.00
Published on Web 02/28/2003

consists of a working electrode composed by a double sheet of ITO (transparent in the range from 350 to 2500 nm) conveniently separated by two Teflon spacers of 0.1 mm. This 0.1 mm separation leads to capillary ascending of the solution. The auxiliary electrode consists of a platinum gauche perpendicularly located with respect to the bottom part of the ITO electrode at an approximate distance of 10 mm. An Ag/Ag^+ reference electrode consisting of a wire located between the reference and the working electrode was used. The three electrodes are assembled in a Teflon sttoper which at the same time covers the solution compartiment. The solution compartment is a 1×1 cm^2 quartz cuvette.

Experimental Procedure. A 1 mL sample of a 0.1 M tetrabutylammonium tetrafluoroborate ($TBABF_4$) solution in CH_2Cl_2 is added to the cuvette which is covered with the three-electrode stopper. When the ITO electrode contacts the solution, the liquid ascends up to the top of the electrode giving rise to an 0.1 mm active layer for spectroscopic measurements. For the case of vis−NIR purposes, the background is recorded only with the electrolyte solution, which is then adequately removed, with an absorbent piece of paper, from the ITO electrode. In the next step the solid oligothiophene is added to the 1 mL solution and conveniently stirred. Saturated solutions are used. Finally, the three-electrode system is again introduced up to contact with the solution. In the case of the Raman experiments, background measurements are not required.

Spectroscopic Measurements. The vis−NIR spectra were obtained with a Perkin-Elmer Lambda 19 spectrometer, recording only one scan per spectrum (highest recording speed of 960 nm/min and a low NIR sensibility to avoid electrolyte interference were used). FT-Raman spectra were measured using an FT-Raman accessory kit (FRA/106-S) of a Bruker Equinox 55 FT-IR interferometer. A continuous-wave Nd:YAG laser working at 1064 nm was employed for Raman excitation. A germanium detector operating at liquid nitrogen temperature was used. Raman scattering radiation was collected in a back-scattering configuration with a standard spectral resolution of 4 cm^{-1}. The power of the laser beam was kept at a level lower than 30 mW, and an average of 150 scans was accumulated.

Theoretical Calculations. All theoretical calculations including geometry optimizations, electronic structures and electronic excitation energies were carried out at the density functional theory (DFT) level using the Becke's three parameter B3LYP exchange−correlation functional[11] and the 3-21G* basis set.[12] Geometry optimizations are performed on isolated entities. The neutral and dication molecules were treated as closed-shell systems, while for the radical cation open-shell system optimizations were carried out using a spin unrestricted wave function (UB3LYP procedure). Vertical electronic excitation energies were computed by using the time-dependent density functional theory (TDDFT).[13,14] The computational cost of TDDFT is roughly comparable to single-excitation theories based on a HF ground state, such a single-excitation configuration interaction (CIS); however, numerical applications reported so far indicate that TDDFT employing current exchange−correlation functional performs significantly better than HF-based single-excitation theories for the low-lying valence excited states of both closed-shell and open-shell molecules.[15,16] All the calculations were performed using the A.7 revision of the Gaussian 98 program package[17] running on a SGI Origin 2000 computer.

III. In Situ Vis−NIR Spectroelectrochemical Study

The cyclic voltammograms (CV) of the BMA-3T and BMA-4T were obtained in CH_2Cl_2 versus Ag/Ag^+ and displayed in Figure 2. The CV of BMA-3T exhibits three reversible

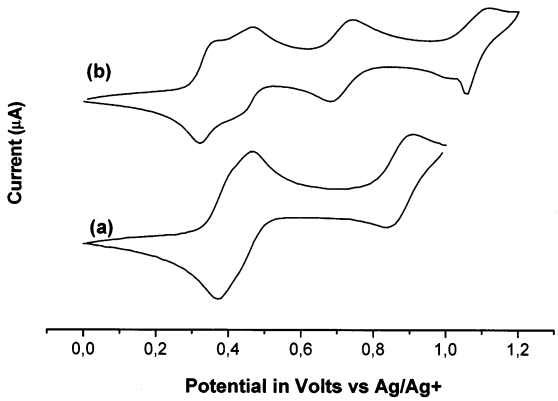

Figure 2. Cyclic voltammetries of (a) BMA-3T and of (b) BMA-4T.

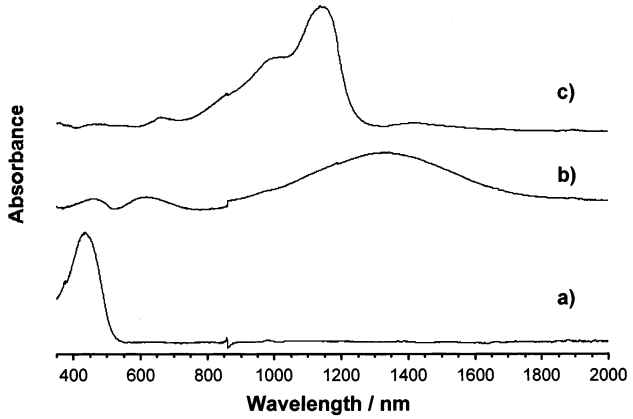

Figure 3. In situ vis−NIR absorption spectra of BMA-3T recorded between 0 and 1.5 V electrochemical range. Parts a−c denote the spectra of the neutral, radical cation, and dication, respectively.

oxidations at 0.393, 0.441, and 0.870 V, while the CV of BMA-4T displays up to four oxidations at 0.347, 0.434, 0.712, and at 1.089 V.[7] In these experimental conditions the reduction peak coupled to the fourth oxidation in BMA-4T shows a large peak current giving rise to an enhanced current "spike" that suggests that the tetracation species precipitates somewhat on the electrode surface when it is formed. We can observe that the oxidation potentials are shifted to lower potential in the largest oligomer, which indicates the existence of certain dependence of the oxidations with the chain length in the sense that charges can be better stabilized or accommodated in the tetramer than in the trimer. On the other hand, the maxima of the $\pi-\pi^*$ band in the electronic absoption spectra of the BMA-nT series are red-shifted as the chain becomes longer, which is also in agreement with the increment of the extension of the π-electron delocalization.[9−10]

Figures 3 and 4 display, respectively, the in situ vis−NIR absorption spectra of BMA-3T and of BMA-4T as a function of the electrochemical doping level. Spectroelectrochemical oxidation of BMA-3T and BMA-4T in 0.1 M $TBABF_4/CH_2Cl_2$ leads to significant changes in the vis−NIR spectral region. One-electron oxidation causes the 442 and 455 nm bands associated to the neutral species of the trimer and of the tetramer, respectively, to disappear as two new bands at 643 and 1323 nm in BMA-3T and at 671 and 1420 nm in BMA-4T grow in intensity. The two-band spectral patterns in both compounds are similar, being characterized by broad features in which the lower energy band intensity is always twice the intensities of the bands around 600−800 nm. These spectral features clearly correspond to the radical cation species on the basis of the data reported in the literature for a large number of monooxidized oligothio-

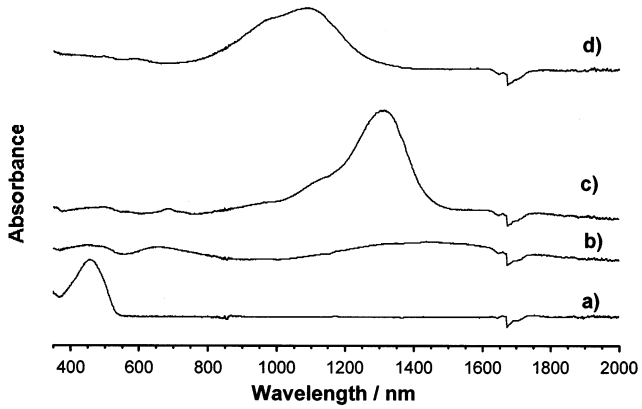

Figure 4. In situ vis−NIR absorption spectra of BMA-4T recorded between 0 and 1.5 V electrochemical range. Parts a−d denote the spectra of the neutral, radical cation, dication, and radical trication, respectively.

phenes.[18−21] Thus, the electronic spectrum of the electrochemically obtained radical cation of 3′,4′-dibutyl-2,5″-diphenyl-2,2′:5′,2″-terthiophene (Ph2-3T^{+}) in 0.1 M $TBAPF_6/CH_2Cl_2$ displays two bands at 654 and at 1106 nm. The comparison of the data reveals great resemblance between the wavelength of the high-energy band of Ph2-3T$^{+\cdot}$ and of the BMA compounds. However, values for the maxima of the low-energy band are rather different. The different topology and contributions of the terminal and of the thiophene core on the frontier orbitals can account for this observation as will be discussed later on.[21,22]

At higher electrochemical potentials the oxidation yields the disappearance of the two-bands above-described and the growth of one intense band at 1150 nm in BMA-3T and at 1309 nm in BMA-4T. By analogy with similar data on oligothiophenes,[23] these spectral features are consistent with the formation of a dication species with a bipolaron structure, for which the two absorption bands of the radical cation are replaced by only one absorption at intermediate energies. The dication species of Ph2-3T (3′,4′-dibutyl-5,5″-diphenyl-2,2′:5′,2″-terthiophene) is not stable; however, the electronic spectrum of the electrochemically obtained dication of Ph2-6T (3′,4′,3‴,4‴-tetrabutyl-5,5‴′-diphenyl-2,2′:5′,2″:5″,2‴:5‴,2⁗:5⁗,2⁗′-sexithiophene) is characterized by the presence of one intense band at 1155 nm.[24] The data suggest the generation of dicationic species in our BMA compounds. Once again, the competitive effect of the different parts of the molecule would account for these facts.[21,22]

Further oxidation of BMA-3T does not produce any significant spectral changes. However, it is noteworthy that a shoulder at 1006 nm is clearly observed which seems to somewhat evolve at increasing potentials, but never becomes a clear band. Electrolysis of BMA-4T at the highest oxidation potentials generates the appearance of a new spectral pattern consisting of one intense band at 1095 nm with a shoulder at 972 nm. To our knowledgement, only a few works exist in the literature about short oligothiophenes mentioning oxidation species higher than a dication.[24,25] In fact, some of us have recorded for the first time the Raman and electronic spectra of a trication, Ph2-6T^{+3}.[24] The electronic spectrum of this species is characterized by the presence of one intense band at 1160 nm and one moderately intense at 999 nm. The absorption spectra of Ph2-6T^{+3} and of the highly oxidized BMA-4T nicely correlate, suggesting the existence of a trication species. At this point, we can tentatively assign the shoulder at 1006 nm in highly oxidized BMA-3T to the trication species which probably has a shorter lifetime than the required time for the experiment.

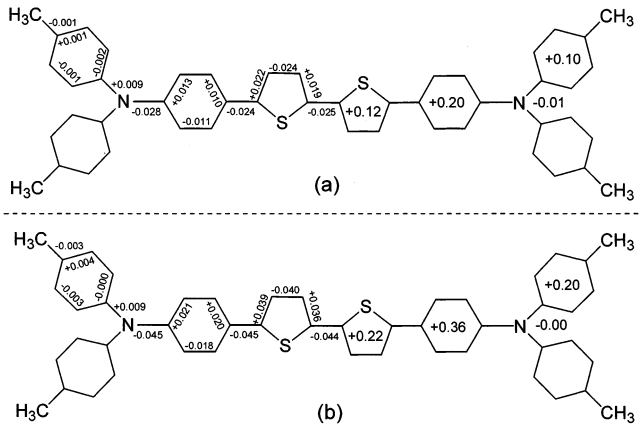

Figure 5. Bond distances and Mülliken atomic charge increment (with respect to the optimized structure of the neutral system) of the (a) radical cation and (b) dication species of BMA-2T, calculated at the B3LYP/3-21G* level.

IV. Theoretical Calculations: Optimized Geometries, Mülliken Atomic Charges, and Electronic Spectra

To better understand the evolution on the electronic absorption and Raman spectra as a function of the doping level, we have computed the optimized geometries and the Mülliken atomic charges in the neutral, radical cation ,and dication species of the BMA-2T at the B3LYP/3-21G* level of calculations. We choose BMA-2T as a model oligomer with a relatively large molecular size, which can reasonably reflect the effect of the ionization on the larger oligothiophenes, with a moderate computational cost. In any case, the theoretical data will be used to underline how the molecular parameters evolve from the neutral to charged species and will serve for providing guidelines to interpret the optical spectra.

The neutral molecule exhibits an aromatic structure in the bithiophene moiety, with a benzenoid character in the phenyl rings. The outermost phenyl rings are largely distorted by 42.4° from the bithiophene moiety which shows an almost planar conformation. Also the phenyl ring between the bithiophene and the nitrogen is distorted by 22.2°. Figure 5 displays the optimized bond lengths and charge increments along the CC path on going from the neutral BMA-2T to its radical cation and dication. The UB3LYP/3-21G* geometry of the radical cation is shifted toward planarity: the value of the torsion angles are reduced to 22.2° and to 3.0°, respectively, for the outer and inner phenyl rings. On the other hand, the bond distances of the original (neutral molecule) double bonds of the central bithiophene and its directly connected phenyl rings are shortened while the bond distances of the original single bonds are lengthened. The amplitude of the structural modifications progresively decrease away from the center of the oligomer. This geometrical evolution from the neutral to the radical cation is consistent with the attainment of a quinoid-like structure in this part of the molecule. After doubly ionization of BMA-2T and with respect to the radical cation the original double bonds get even shorter and the single ones larger, indicating that a more accentuated quinoid-like structure in the central bithiophene and the inner phenyl rings is predicted. The largest bond distance change is calculated for the central CC bond that connects the two thiophene rings: 1.442 Å in the neutral, 1.419 Å in the radical cation, and 1.398 Å in the dication. This theoretical data reveals that the quinoid structure is centered at the midle of the molecule. Furthermore, it is worth mentioning that the bond distance connecting the nitrogen and the inner phenyl ring shortens from 1.419 Å in the neutral to 1.391 Å in the radical

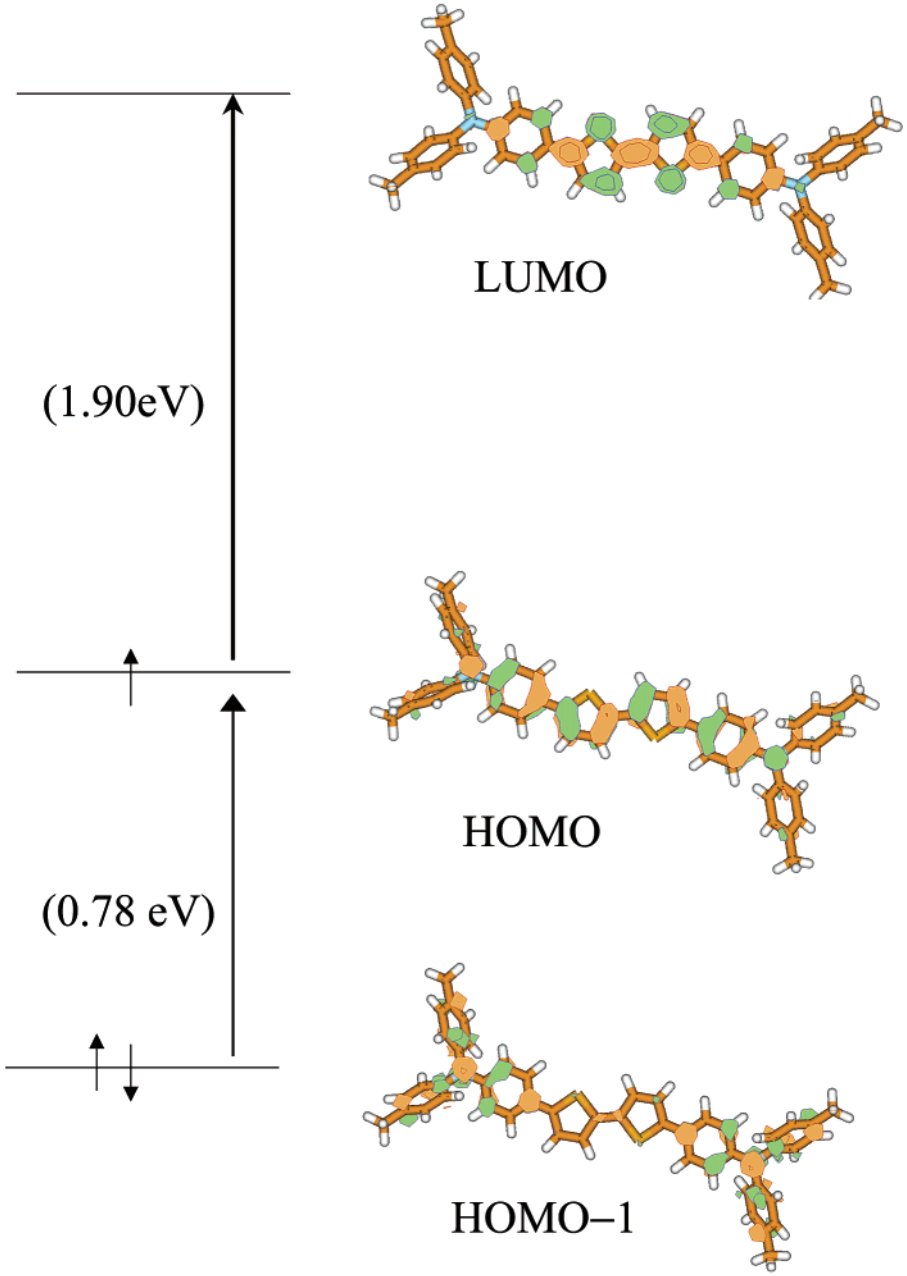

Figure 6. Electronic density contours calculated for the HOMO-1, HOMO, and LUMO of the radical cation of BMA-2T at the UB3LYP/3-21G* level. In parentheses, calculated values for each transition.

cation and to 1.374 Å in the dication, while the other C−N bonds remain almost unchanged.

Let us briefly summarize the main changes in the atomic charges after ionization (see Figure 5). In view of the B3LYP/3-21G* Mülliken atomic charges, some general considerations can be made: (a) the nitrogen atoms scarcely change their negative charges; (b) the overall charge over the inner phenyl rings varies from +0.27 *e* in the neutral oligomer to +0.47 *e* in the radical cation and to +0.60 *e* in the dication; and (c) the central bithiophene is also extensively charged upon ionization: −0.06 *e* in the neutral, +0.20 *e* in the radical cation, and to +0.42 *e* in the dication. Summing up, we can conclude that the ionization mainly affects to the bithiophene moiety and to the inner phenyl rings, and that the positive charges are mainly located over the inner phenyl rings.

Vertical electronic excitation energies were carried out by using the time-dependent density functional theory (TDDFT).[13,14] Electronic spectra were computed at the B3LYP/3-21G* level using the optimized geometries discussed above. For the neutral BMA-2T, calculations reproduce the existence of only one allowed electronic transition at 2.72 eV (456 nm), with oscillator strengths *f* of 1.78, which corresponds to the transition to the first excited state and is mainly described by a one-electron excitation from the highest occupied molecular orbital (HOMO) to the lowest unoccupied molecular orbital (LUMO). The experimental absorption at 2.81 eV and at 2.73 eV in BMA-3T and in BMA-4T, respectively, is therefore assigned to the HOMO → LUMO one-electron promotion calculated at 2.72 eV in BMA-2T. The topological analysis of the HOMO and LUMO orbitals reveals that these orbitals are of π nature and are mainly concentrated in the bithiophene backbone with an important contribution of the inner phenyl rings and of the nitrogen atoms. This conjugative effect from the terminal groups can account for the high wavelength position of the maximun of the electronic band in our compounds with

respect to nonsubstituted quaterthiophenes, quinquethiophenes, and sexithiophenes or diphenyl-substituted sexithiophenes.[18−20]

The electronic spectrum of BMA-2T$^{+\cdot}$ was computed at the UB3LYP/3-21G* level using TDDFT approach. Theoretical calculations predict the occurrence of two intense electronic transitions at 0.78 eV ($f = 0.95$) and 1.90 eV ($f = 0.99$). The calculated spectrum is in good agreement with the two absorption bands observed experimentally for the low-oxidized species of BMA-3T and BMA-4T. Frontier orbitals for BMA-2T$^{+\cdot}$ are sketched in Figure 6 as a prototypical case, whereas the frontier orbitals for the neutral and for the dication will be given upon request to the authors. The experimental bands at 1.93 eV and at 1.85 eV in the low-oxidized species of BMA-3T and of BMA-4T, respectively, correlate with the theoretical transition at 1.90 eV which mainly corresponds to an electronic excitation from the singly occupied HOMO to the LUMO. As seen before, this electronic absorption appears at very similar wavelength in our compounds and in Ph2-3T$^{+\cdot}$ which can be explained by the fact that this transition takes place from orbitals that are mainly located at the thiophene backbone (see HOMO in Figure 6). Second, the band experimentally observed at 0.94 eV and at 0.87 eV for the low-oxidized species of BMA-3T and of BMA-4T, which are red-shifted with respect to that measured for the radical cation of Ph2-3T,[18] correlates with the electronic transition calculated at 0.78 eV and mainly corresponds to an transition from the doubly occupied HOMO-1 to the HOMO orbitals. The analysis of these two orbital indicates that the HOMO-1 orbital is mainly concentrated in the terminal groups with an almost negligible participation of the thiophene spine. The almost exclusive involvement of the BMA groups in this transition can account for the above-mentioned red-shifting. Another remark about this transition is that has important contributions from other monoelectronic promotions what can give rise to a certain transition overlapping and to a broadening of the experimental associated feature as is nicely observed in the spectra.

Finally, the electronic spectrum of BMA-2T^{+2} was computed at the B3LYP/3-21G* level. Below 2 eV, calculations predict that only an intense transition is dipole-allowed and is calculated at an energy of 1.20 eV ($f = 2.71$) intermediate between those obtained for the radical cation in good accord with the experiment. This transition is assigned to an HOMO → LUMO monoelectronic promotion and can be related to the electronic bands experimentally measured at 1.08 eV and at 0.95 eV in the higher oxidized species of BMA-3T and BMA-4T, respectively. Chemical model predicts this band to be almost 3 times more intense than the bands in the BMA-2T$^{+\cdot}$ which is also observed in the experimental spectra. Particularly for the dication of BMA-4T, this band is red-shifted with respect to that of Ph2-6T^{+2} (1.08 eV).[24] The poor involvement of the bithiophene core in the HOMO of the dication can establish relevant differences with respect to the sexithiophene and thus can reasonably account for this experimental observation.

At this point, calculations guide well the assignment of the electronic spectra and reveals relevant influence of the terminal groups in the structure of the oxidized species. Furthermore, this theory−experiment comparison leads to help the interpretation of the Raman spectra which allows us, on the other hand, to obtain deeper information about molecular and geometrical parameters.

V. In Situ Raman Spectroelectrochemical Study

The inspection of the Raman spectra of the oxidized species brings us the opportunity of relating the vibrational features with the different interplay or participation of the thiophene backbone, the inner phenyl rings and the outermost BMA groups in the electronic structure of the charged defects. This is a difficult task to address merely from the study of the electronic spectra and gives us information about how chemical functionalization strategies can be used to improve organic-based materials.

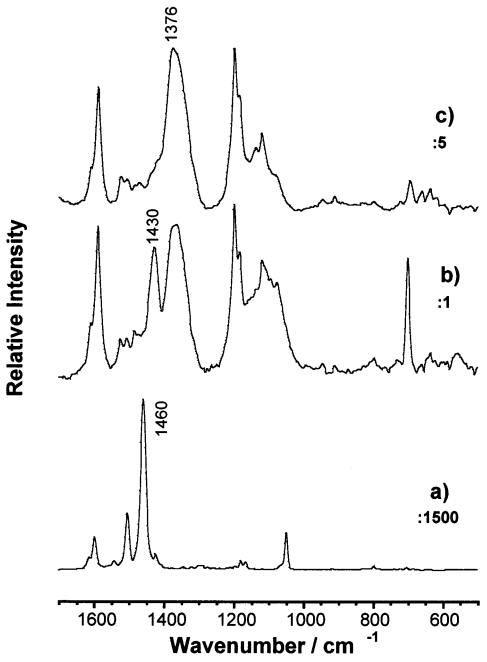

Figure 7. In situ FT-Raman spectra of the electrochemically generated (b) radical cation and (c) dication species of BMA-3T. The spectrum labeled as (a) corresponds to the neutral species in solid state. Numerical values in bold refer to the relative intensity with respect to that of spectrum (b).

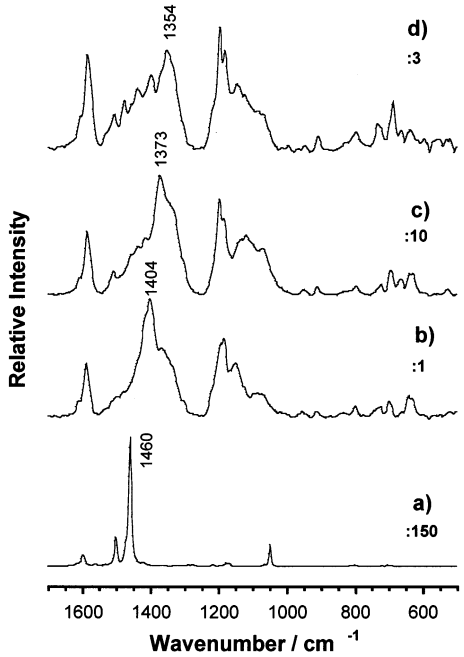

Figure 8. In situ FT-Raman spectra of the electrochemically generated (b) radical cation, (c) dication and (d) radical trication species of BMA-4T. The spectrum labeled as (a) corresponds to the neutral species in solid state. Numerical values in bold refer to the relative intensity with respect to that of spectrum (b).

V.a. Raman Bands Associated to the Terminal Groups. Figures 7 and 8 display the in situ Raman spectra of BMA-3T

TABLE 1: Wavenumber Values (in cm^{-1}) Measured for the Raman Bands in the Range 1700−1000 cm^{-1} for the Neutral BMA-3T (as Solid) and for the Electrochemically Generated Radical Cation and Dication, in 0.1 M $TBABF_4$ in CH_2Cl_2

neutral	radical cation	dication
1614	1608	1608
1599		
	1591	1591
	1525	1525
1505	1505	1505
	1485	
	1473	1473
1460		
		1457
	1444 sh[a]	
	1430	1436 sh
1424		
		1418 sh
	1375	1376
	1364	1364 sh
	1352	1344 sh
	1335	1321 sh
	1318	
	1200	1200
1180	1186	1186
1167		
	1137	1137
	1120	1120
	1084	1100 sh
	1077	1083 sh
1050		

[a] sh means a shoulder band.

TABLE 2: Wavenumber Values (in cm^{-1}) Measured for the Raman Bands in the Range 1700−1000 cm^{-1} for the Neutral BMA-4T (as Solid) and for the Electrochemically Generated Radical Cation, Dication, and Radical Trication, in 0.1 M $TBABF_4$ in CH_2Cl_2

neutral	radical cation	dication	radical trication
1616	1608	1608	1608
1598	1588	1588	1588
			1515 sh
	1510	1510	1510
1502			
			1479
1460			
		1457	1457 sh
	1437 sh[a]	1437	1440
1422			
	1415 sh	1415	
	1404		1396
	1370	1373	1373 sh
	1340 sh	1345 sh	1354
			1337 sh
	1300 sh	1306 sh	1300 sh
	1222 sh		1217 sh
	1197	1200	1200
1178	1186	1184	1184
1170			
	1153		
		1147 sh	1150
		1136	1141 sh
	1127	1122	1125
	1086		1088
		1072	1072
1050			

[a] sh means a shoulder band.

and of BMA-4T as a function of the electrochemical doping level and obtained with a laser excitation line working at 1064 nm. Because of the samples show intense electronic absorption bands in the NIR region close to 1064 nm, most of the Raman spectra were taken in resonant condictions what will explain the large intensity of the spectra as well as the different intensity ratio of ones species with respect to others. Finally, Tables 1 and 2 summarize the values for the Raman bands, obtained at different oxidation levels.

The Raman profiles of BMA-3T and BMA-4T suddenly change with respect to those of the neutral materials upon electrochemical oxidation. It is observed that some intense bands do not change their frequencies as electrochemical oxidation progresses from the neutral to the radical cation, dication, or radical trication. Let us examine in three groups the behavior of these bands:

(i) Bands at 1608 cm^{-1} in oxidized BMA-3T and at 1610 cm^{-1} in oxidized BMA-4T correlate respectively with the band at 1614 cm^{-1} in neutral BMA-3T and with the band at 1616 cm^{-1} in neutral BMA-4T; thus, they can be assigned to ν(C═C) stretching vibrations mainly located at the outermost phenyl rings. The 6 cm^{-1} downshift reflects that these groups are somewhat affected by the doping which could be accounted for the planarization of the tolyl groups (with respect to the central backbone) facilitating conjugation of the BMA groups with the central phenyl/thiophene backbone. On the other hand, the increase of the overall charge on the tolyl groups (+0.32 *e* in the neutral, +0.42 *e* in the radical cation, and +0.53 *e* in the dication, according to the B3LYP/3-21G* Mülliken atomic charges calculated for BMA-2T model), could account for the large increment of the Raman intensity of these phenyl-associated vibrations with respect to those observed in the neutral system.

(ii) Bands at 1591 cm^{-1} in oxidized BMA-3T and at 1588 cm^{-1} in oxidized BMA-4T are related with the bands in the neutral species at 1599 cm^{-1} in BMA-3T and at 1598 cm^{-1} in BMA-4T; thus, they can be assigned to the ν(C═C) stretching vibrations mainly located at the inner phenyl groups.[10] The frequency downshift by 8 cm^{-1} in BMA-3T and by 10 cm^{-1} in BMA-4T are mainly due to the quinoidization of these phenyl rings on going from the neutral to the radical cation as reflected by the DFT calculations (Figure 5). According to the model, there occurs an relevant planarization of the inner phenyl rings with respect to the bithiophene moiety when ionization progresses: the $C-C_{phenyl}-C-C_{thiophene}$ dihedral angle varies from 22.2° in the neutral species up to 0.9° in the dication (3.0° in the radical cation). Zerbi et al. have demonstrated that the planarization of the biphenyl molecule little affects the force field in the sense that the ν(C═C) frequencies of the phenyl

rings do not change after full planarization with respect to those calculated for the distorted disposition,[26] which is in accordance with the experimental finding that the ν(C═C) phenyl frequencies are little affected by the electrochemical oxidation, and subsequent planarization. Finally, the Raman intensity of the phenyl bands relative to those of the neutral and of the bulk vibrations in the oxidized species significantly increases with the increasing oxidation level. This can be theoretically well-accounted for the fact that phenyl groups support larger positive charge as oxidation level increases (+0.27 *e* in the neutral, +0.47 *e* in the radical cation, and +0.63 *e* in the dication in BMA-2T).

(iii) Very intense dispersions at 1200 cm^{-1} and at 1184−1186 cm^{-1} appear in the Raman spectra of all the oxidized species of BMA-3T and BMA-4T. The spectral behavior of these bands consists of two main features: (a) their frequencies are almost insensitive to the oxidation level and to the length of the thiophene backbone and (b) they display the same intensity ratio relative to the bands around 1610 and 1590 cm^{-1}. Consequently, they can be assigned to vibrations located at the outer and at the inner phenyl groups.

The C−N stretching vibrations of the side groups have been assigned to the bands at 1274, 1293, and 1320 cm^{-1} in the infrared spectra of BMA-3T and BMA-4T.[10] It is largely accepted that some infrared-active vibrations of the neutral oligothiophenes can become Raman-active vibrations after oxidation due, among other factors, to the symmetry breakdown that takes place after electron extractions. This could be the case of the bands around 1310, 1320, 1344, and 1360 cm^{-1} in the oxidized species of BMA-3T and BMA-4T. The general frequency increment with respect to the frequency values of the infrared bands in the neutral species could be ascribed to the strengthening of the C−N bonds connected to inner phenyl rings as predicted by the calculations: 1.419 Å in the neutral, 1.391 Å in the radical cation, and 1.374 Å in the dication of BMA-2T.

V.b. Raman Bands Associated to the Thienyl Backbone. To recognize the Raman bands associated to almost pure thiophene vibrations, Figure 9 displays the Raman spectra of the dicationic species of α, α′-dimethyl sexithiophene[27] (methyl groups do not have much influence in the stabilization of the charged species), α,α′-diphenyl quaterthiophene,[28] and of the dicationic species of BMA-4T. The Raman spectra of the methyl sexithiophene is dominated by the presence of one strong band at 1415 cm^{-1} that has been assigned to an in-phase CC stretching of the thiophene rings, whereas in the spectrum of the diphenyl quaterthiophene points out the Raman dispersion at 1431 cm^{-1}, also assigned to an in-phase CC stretching of the thiophene rings somewhat coupled with the vibration of the terminal phenyl caps, whose ν(C═C) Raman frequency bands are downshifted by 6 cm^{-1} with respect to the neutral system.[28] These data well-agree with the 8 cm^{-1} downshift described for the ν(C═C) vibrations of the inner phenyl rings on going from the neutral to the oxidized species of BMA-3T and BMA-4T.

The comparison of the Raman spectra of the dicationic BMA-3T and BMA-4T with those of the dication of α,α′-dimethyl sexithiophene reveals that the bands in the spectral range of 1350−1500 cm^{-1} are due to vibrations mainly emerging from the thiophene backbone. In fact, these vibrations do show dependence of the band peak position with the oxidation level as has been previously shown in oligothiophenes, i.e., the most intense band of the neutral species of α,α′-dimethyl sexithiophene appears at 1477 cm^{-1}, while for its radical cation and dication appear at 1438 and 1415 cm^{-1}, respectively,[27] or at 1460 cm^{-1} in the neutral α,α′-diphenylquaterthiophene and at 1440 and 1431 cm^{-1} in its radical cation and dication, respectively.[28]

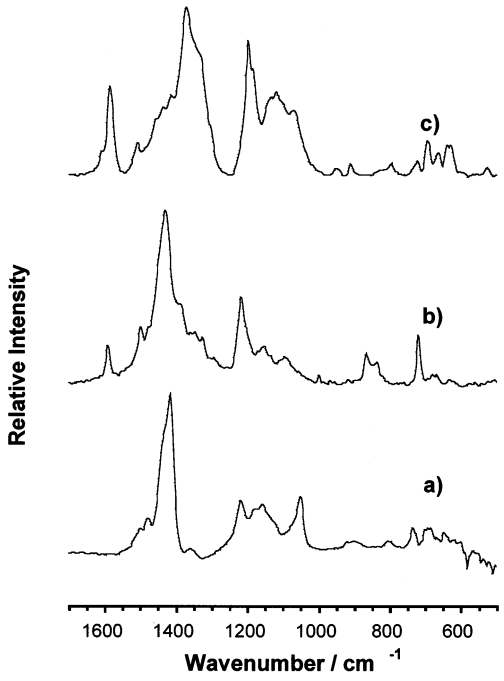

Figure 9. Raman spectra of the dicationic species of (a) α,α′-dimethyl sexithiophene, (b) α, α′-diphenyl quaterthiophene, and (c) BMA-4T.

After one-electron extraction, intense bands at 1430 cm^{-1} (shoulder at 1444 cm^{-1}) in BMA-3T and at 1404 cm^{-1} (shoulders at 1415 and at 1437 cm^{-1}) in BMA-4T appear. These two bands can be correlated with the most intense Raman bands in the neutral species at 1460 cm^{-1} in BMA-3T and in BMA-4T and described as ν(C═C) stretching vibrations.[10] The most pronounced bond length changes take place in the oligothiophene backbone; thus, the dication of BMA-2T the central bithiophene acquires a clearly quinoid caracter. This evolution from an aromatic structure (neutral state) to a quinoid structure in the oxidized species means that the C═C double bonds are weakened, whereas the C−C single ones are strengthened. Furthermore, this quinoid structure is more pronounced in the higher oxidized species. Consequently, vibrations mainly associated to C═C stretching vibrations in the neutral system downshift their frequencies, such as those at 1460 cm^{-1} that now appear at 1430 cm^{-1} in the radical cation of BMA-3T and at 1404 cm^{-1} in the radical cation of BMA-4T.

Upon second extraction, the most intense Raman bands associated with thiophene vibrations appear at 1376 cm^{-1} in BMA-3T and at 1373 cm^{-1} in BMA-4T. As mentioned before the increment of the quinoid character of the thiophene rings can accounted for this larger downshift of the originally ν(C═C) vibrations in the dication with respect to the radical cation. The third electron-extraction in the case of the BMA-4T leads to a even larger downshift of the most intense Raman band associated with thiophene CC stretching vibrations, thus appearing at 1354 cm^{-1}. The dynamic analysis in these highly charged molecule becomes difficult, so a few more vibrations probably due to the thiophene backbone CC stretchings are observed at 1510, 1479, and 1457 cm^{-1} in the higher oxidized species of BMA-4T, whereas the bands at 1373, 1390, and 1440 cm^{-1}, which are common to all the oxidized species, probably arise from CC vibrations mainly located at the thiophene backbone.

Finally, we would mention the multiplets of bands at 1217 (shoulder of the band at 1200 cm^{-1}), 1140−1150, 1120−1127, and 1070−1080 cm^{-1}. These bands correlate with the multiplet

of bands at 1219, 1157, and 1051 cm^{-1} in the dicationic species of α,α′-dimethyl sexithiophene and therefore associated with thiophene vibrations.[27] In oxidized oligothiophenes, these bands are always weaker than the Raman bands around 1400 cm^{-1} and increase their intensity with the increasing oxidation level which is also observed in the Raman spectra of the oxidized species of BMA-3T and of BMA-4T.

VI. Conclusions

In situ electronic absorption (vis−NIR range) and in situ FT-Raman spectra demonstrate the generation of a radical cation and a dication species in BMA-3T, whereas in BMA-4T up to a radical trication is stabilized by the oligothiophene compound. The low-energy band of the electronic spectra of the charged species in the BMA compounds is red-shifted with respect to those of the oligothiophenes reported in the literature what has been interpreted on the basis of the topology of the frontier orbitals which at the same time reveals the stabilizing effect of the terminal groups in the description of the oxidized species of the studied compounds.

The large Raman intensity of the oxidized species are accounted by resonance Raman effects and clearly indicates that the assigned vibrations are strongly coupled with the HOMO−LUMO electronic transitions which, on the other hand, back up the use of the Raman spectroscopy to obtain useful information about the electronic structure of the oxidized molecules. The Raman spectra of the oxidized species are dominated by bands arising from the tolyl and from the inner phenyl rings. This supports the hipothesis of the large stabilization that the tolyl groups and the inner phenyl groups exert upon the oxidized species. Surpringly, these bands dominate the whole Raman spectra, which is a new feature because of the vibrations associated to the thiophene rings are usually the most intense. Finally, the bands corresponding to vibrations located over the thiophene rings are nicely correlated as a function of the electrochemical doping level and are the unique spectroscopic marker useful for detecting the presence of radical cation, dication, or radical trications.

This study shows how the electronic structure of the oligothiophene backbone can be modulated by suitable modification or substitution with rich electron terminal groups, such as 4-[bis-(4-methylphenyl)amino] phenyl groups. Furthermore we have presented meaningful data about charged defects in the BMA compounds which can be viewed as model systems for hole carriers or photoexcitations in the real FET or LED.

Acknowledgment. The present work was supported in part by the Dirección General de Enseñanza Superior (DGES, MEC, Spain) through the research project BQU2000-1156. We are also indebted to Junta de Andalucía (Spain), funding for our research group (FQM-0159). J.C. is grateful to the Ministerio de Ciencia y Tecnología for a Ramón y Cajal position of Chemistry at the University of Málaga.

References and Notes

(1) Katz, H. E.; Bao. Z.; Gilat, S. L. *Acc. Chem. Res*. **2001**, *34*, 359−369.

(2) Makinen, A. J.; Hill, I. G.; Kinoshita, M.; Noda, T.; Shirota, Y.; Kafafi, Z. H. *J. App. Phys*. **2002**, *9*, 5456−5461; Makinen, A. J.; Hill, I. G.; Noda, T.; Shirota, Y.; Kafafi, Z. H. *Appl. Phys. Lett.* **2001**, *78*, 670.

(3) Cocchi, M.; Virgili, D.; Giro, G.; Fattori, V.; Di Marco, P.; Kalinowski, J.; Shirota *Appl. Phys. Lett*. **2002**, *80*, 2401−2404. Giebeler, C.; Antoniadis, H.; Bradley, D. D. C.; Shirota, Y. *J. App. Phys*. **1999**, *85*, 608−616. Shirota, Y. *J. Mater. Chem*. **2000**, *10*, 1.

(4) Horowitz, G.; Fichou, D.; Peng, X.; Garnier, F. *Solid State Commun*. **1989**, *72*, 381.

(5) Granstrom, M.; Petrisch, K.; Arias, A. C.; Lux, A.; Andersson, M. R.; Friend, R. H. *Nature* **1998**, *395*, 257.

(6) Pappenfus, T. M.; Cherterfield, R. J.; Frisbie, C. D.; Mann, K. R.; Casado, J.; Raff, J. D.; Miller, L. L. *J. Am. Chem. Soc*. **2002**, *124*, 4184−4186.

(7) Noda, T.; Imae, I.; Noma, N.; Shirota, Y. *Adv. Mater*. **1997**, *9*, 239.

(8) Noda, T.; Ogawa, H.; Noma, N.; Shirota, Y. *Adv. Mater*. **1997**, *9*, 720. Noda, T.; Ogawa, H.; Noma, N.; Shirota Y. *App. Phys. Lett*. **1997**, *70*, 699.

(9) Noda, T.; Ogawa, H.; Noma, N.; Shirota, Y. *J. Mater. Chem*. **1999**, *9*, 2177.

(10) Moreno Castro, C.; Ruiz Delgado, M. C.; Hernandez, V.; Shirota, Y.; Casado, J.; Lopez Navarrete, J. T. *J. Phys. Chem. B* **2002**, *106*, 7163.

(11) Rauhut, G.; Pulay, P. *J. Phys. Chem*. **1995**, *99*, 3093.

(12) Francl, M. M.; Pietro, W. J.; Hehre, W. J.; Binkley, J. S.; Gordon, M. S.; Defrees, D. J.; Pople, J. A. *J. Chem. Phys.* **1982**, *77*, 3654.

(13) Gross, E. K. U.; Kohn, W. *Adv. Quantum Chem*. **1990**, *21*, 255. Gross, E. K. U.; Ullrich, C. A.; Gossmann, U. J. In *Density Functional Theory*; Gros, E. K. U., Driezler, R. M., Eds.; Plenum Press: New York, 1995; p 149.

(14) Casida, M. E. In *Recent Advances in Density Functional Methods, Part I*; Chong, D. P., Ed.; World Scientific: Singapore, 1995; p 155.

(15) Wiberg, K. B.; Stratmann, R. E.; Frisch, M. J. *Chem. Phys. Lett.* **1998**, *297*, 60. Stratmann, R. E.; Scuseria, G. E.; Frisch, M. J. *J. Chem. Phys.* **1998**, *109*, 8218. Hirata, S.; Lee, T. J.; Head-Gordon, M. *J. Chem. Phys.* **1999**, *111*, 8904. Hsu, C.-P.; Hirata, S.; Head-Gordon, M. *J. Phys. Chem. A* **2001**, *105*, 451.

(16) Casado, J.; Miller, L. L.; Mann, K. R.; Pappenfus, T. M.; Kanemitsu, Y.; Ortí, E.; Viruela, P. M.; Pou-AméRigo, R.; Hernández, V.; López-Navarrete, J. T. *J. Phys. Chem. B* **2002**, *106*, 3872.

(17) Frisch, M. J.; Trucks, G. W.; Schlegel, H. B.; Scuseria, G. E.; Robb, M. A.; Cheeseman, J. R.; Zakrzewski, V. G.; Montgomery, J. A.; Stratman, R. E.; Burant, S.; Dapprich, J. M., Millam, J. M.; Daniels, A. D.; Kudin, K. N.; Strain, M. C.; Farkas, O.; Tomasi, J.; Barone, V.; Cossi, M.; Cammi, R.; Mennucci, B.; Pomelli, C.; Adamo, C.; Clifford, S.; Ochterski, G.; Petersson, A.; Ayala, P. Y.; Cui, Q.; Morokuma, K.; Malick, D. K.; Rabuck, A. D.; Raghavachari, K.; Foresman, J. B.; Cioslowski, J.; Ortiz, J. V.; Stefanov, B. B.; Liu, G.; Liashenko, A.; Piskorz, I.; Komaromi, I.; Gomperts, R.; Martin, R. L.; Fox, D. J.; Keith, T.; Al-Laham, M. A.; Peng, C. Y.; Manayakkara, A.; Gonzalez, C.; Challacombe, M.; Gill, P. M. W.; Johnson, B. G.; Chen, W.; Wong, M. W.; Andres, J. L.; Head-Gordon, M.; Replogle, E. S.; Pople, J. A. *Gaussian 98*, revision A.1; Gaussian, Inc.: Pittsburgh, PA, 1998

(18) Graf, D. D.; Campbell, J. P.; Mann, K. R.; Miller L. L. *J. Am. Chem. Soc.* **1996**, *118*, 5480; Graf, D. D.; Duan, R. G.; Campbell, J. P.; Miller, L. L.; Mann, K. R. *J. Am. Chem. Soc*. **1997**, *119*, 5888.

(19) Bauerle, P.; Segelbacher, U.; Maier, A.; Mehring, M. *J. Am. Chem. Soc.* **1993**, *115*, 10217; Bauerle, P.; Fisher, T.; Bidlingmeier, B.; Stabel, A.; Rabe, J. *Angew. Chem., Int. Ed. Engl*. **1995**, *34*, 303.

(20) Hotta, S.; Waragai, K. *J. Phys. Chem*. **1993**, *29*, 7427. Zotti, G.; Schiavon, G.; Berlin, A.; Pagani, G. *Chem. Mater*. **1993**, *5*, 430.

(21) Cornil, J.; Gruhn, N. E.; dos Santos, D. A.; Malagoli, M.; Lee, P. A.; Barlow, S.; Thayumanavan, S.; Marder, S. R.; Armstrong, N. R.; Bredas, J.−L. *J. Phys. Chem. A* **2001**, *105*, 5206−5211.

(22) Malagoli, M.; Bredas, J.-L. *Chem. Phys. Lett.* **2000**, *327*, 13−17. Coropceanu, V.; Malagoli, M.; Andre, J. M.; Bredas, J.−L. *J. Chem. Phys.* **2001**, *115*, 10409−10416.

(23) Van Haare, J. A. E. H.; Havinga, E. E.; van Dogen, J. L. J.; Janssen, R. A. J.; Cornil, J.; Bredas, J.-L. *Chem. Eur. J*. **1998**, *4*, 1509.

(24) Pappenfus, T. M.; Mann, K. R. Unpublished results. Casado, J.; Miller, L. L.; Mann, K. R.; Pappenfus, T. M.; Hernandez, V.; Lopez Navarrete, J. T. *J. Phys. Chem. B* **2002**, *106*, 3597−3606.

(25) Jestin, I.; Frere, P.; Mercier, N.; Levillain, E.; Stievenard, D.; Roncali, J. *J. Am. Chem. Soc.* **1998**, *120*, 8150. Elandaloussi, E. H.; Frere, P.; Richomme, P.; Orduna, J.; Garin, J.; Roncali, J. *J. Am. Chem. Soc*. **1997**, *119*, 10774.

(26) Zerbi, G.; Sandroni, S. *Spectrochim. Acta* **1968**, *24A*, 483; **1968**, *24A*, 511.

(27) Casado, J.; Hernandez, V.; Hotta, S.; Lopez Navarrete, J. T. *Adv. Mater*. **1998**, *10*, 1458. Hernández, V.; Casado, J.; Ramírez, F. J.; Zotti, G.; Hotta, S.; López Navarrete, J. T. *J. Chem. Phys.* **1996**, *104*, 9271.

(28) Casado, J.; Hernandez, V.; Hotta, S.; Lopez Navarrete, J. T. *Synth. Met*. **2001**, *119*, 305−306; Moreno Castro, C.; Ruiz Delgado, M. C.; Hernández, V.; Hotta, S.; Casado, J.; López Navarrete, J. T. *J. Chem. Phys.* **2002**, *116*, 10419.